Self-consistent density functional calculation of the image potential at a metal surface

2007 J. Phys.: Condens. Matter 19 266008

(http://iopscience.iop.org/0953-8984/19/26/266008)

IOP PUBLISHING JOURNAL OF PHYSICS: CONDENSED MATTER

J. Phys.: Condens. Matter **19** (2007) 266008 (10pp) doi:10.1088/0953-8984/19/26/266008

Self-consistent density functional calculation of the image potential at a metal surface

J Jung[1], J E Alvarellos[1], E Chacón[2] and P García-González[1]

[1] Departamento de Física Fundamental, Universidad Nacional de Educación a Distancia, Apartado 60141, 28080 Madrid, Spain
[2] Instituto de Ciencias de Materiales de Madrid, Consejo Superior de Investigaciones Científicas, E-28049 Madrid, Spain

E-mail: jeil@physics.utexas.edu (J Jung)

Received 2 March 2007, in final form 13 May 2007
Published 15 June 2007
Online at stacks.iop.org/JPhysCM/19/266008

Abstract

It is well known that the exchange–correlation (XC) potential at a metal surface has an image-like asymptotic behaviour given by $-1/4(z - z_0)$, where z is the coordinate perpendicular to the surface. Using a suitable fully non-local functional prescription, we evaluate self-consistently the XC potential with the correct image behaviour for simple jellium surfaces in the range of metallic densities. This allows a proper comparison between the corresponding image-plane position, z_0, and other related quantities such as the centroid of an induced charge by an external perturbation. As a by-product, we assess the routinely used local density approximation when evaluating electron density profiles, work functions, and surface energies by focusing on the XC effects included in the fully non-local description.

1. Introduction

The Kohn–Sham (KS) formulation [1] of density functional theory (DFT) [2] is presently the method of choice to evaluate ground-state properties in condensed matter physics. Under this KS formulation, the key quantity is the so-called exchange–correlation (XC) energy functional, $E_{\mathrm{XC}}[n]$, where the main part of the quantum many-body effects are included. However, in actual calculations such a functional must be approximated [3, 4]. Fortunately, and this is the main reason for the popularity of the KS-DFT, simple prescriptions like the local density approximation (LDA) [1] or the generalized gradient approximation (GGA) [5, 6] provide accurate results when evaluating the structural properties of a wide variety of systems. On the other hand, the *static* implementation of the KS method is also the routine starting point for the theoretical study of *excited-state* properties, either using the time-dependent extension of DFT or many-body perturbation theory [7, 8]. This requires accurate KS eigenfunctions

and eigenenergies or, equivalently, a functional approximation to $E_{\rm XC}[n]$ exhibiting a well-behaved functional derivative (XC potential) $v_{\rm XC}(\mathbf{r})$. The commonly used LDA and GGA are rather crude approximations to the actual XC energy functional because the highly non-local and non-analytical character of the electron–electron correlations (in the sense that they do not depend trivially on the electron density) are not described at all by these models. This limitation is evident when analysing the corresponding XC potentials and, as a consequence, there have been numerous attempts to formulate better approximations to the XC functional. These non-local prescriptions are built either by including more sophisticated dependences on the electron density [9–16] or, more recently, by incorporating suitable dependences on the KS eigenfunctions and eigenenergies themselves [17–22].

One of the most evident signatures of the non-local character of the XC functional is the fact that the XC potential $v_{\rm XC}(\mathbf{r})$ exhibits an image-like asymptotic behaviour at a metal surface, $-1/4(z - z_0)$ (z being the coordinate perpendicular to the surface and z_0 the location of the effective image plane) [23, 24]. Although it seems that such a behaviour has minor importance when evaluating ground-state properties [25, 26], its proper description is definitely needed to study problems like tunnelling [27, 28] or surface image states [29–31]. Therefore, the search for a DFT scheme able to provide this image-like decay has been a challenge for many years [32–37], not only to avoid the inclusion of empirical ad hoc procedures in theoretical surface physics [38], but also due to its basic interest in DFT foundations. Only recently, García-González *et al* proposed a method based on a physically well motivated modification of the so-called weighted density approximation (WDA), which we called *momentum*-WDA (mWDA), fulfilling this important property [15, 16]. However, no systematic analysis of results based on self-consistent calculations had been carried out, hence making impossible a complete assessment of this novel functional model. This is the main objective of the present paper.

This paper is structured as follows. After a brief summary of the theory (section 2), we will present fully self-consistent mWDA-KS calculations of simple jellium surfaces in the range of metallic densities ($r_{\rm s} = [3/(4\pi n)]^{1/3} = 2$–$6$, n being the jellium density). In section 3 we will focus on the structural properties (electron density, work function and surface energy) whereas section 4 will be devoted to a detailed discussion of the image-like behaviour of the XC potential. The corresponding conclusions will close this paper. Hartree atomic units will be used throughout the paper, unless otherwise specified.

2. Theory

It is well known that the XC energy functional can be written as

$$E_{\rm XC}[n] = \int {\rm d}\mathbf{r}\, n(\mathbf{r})\, \varepsilon_{\rm XC}(\mathbf{r}) = \int {\rm d}\mathbf{r}\, n(\mathbf{r}) \int {\rm d}\mathbf{r}'\, \frac{n(\mathbf{r}')\, G(\mathbf{r}, \mathbf{r}')}{2\,|\mathbf{r}' - \mathbf{r}|}, \tag{1}$$

where $\varepsilon_{\rm XC}(\mathbf{r})$ is the XC energy per particle at a point $\mathbf{r}$, and $G(\mathbf{r}, \mathbf{r}')$ is the integrated pair correlation function (ipcf). The LDA and extensions thereof are based on the functional modelization of $\varepsilon_{\rm XC}(\mathbf{r})$. In contrast, the WDA [9, 10, 12] uses the hypothesis that, for any inhomogeneous electron system, the ipcf can be constructed from a scaling of the ipcf of an homogeneous electron gas with density n, $G_{\rm hom}(n, |\mathbf{r} - \mathbf{r}'|)$. Specifically,

$$G(\mathbf{r}, \mathbf{r}') \simeq G_{\rm hom}(\tilde{n}(\mathbf{r}), |\mathbf{r}' - \mathbf{r}|), \tag{2}$$

where the *weighted density* $\tilde{n}(\mathbf{r})$ is obtained by imposing the sum rule

$$\int {\rm d}\mathbf{r}'\, n(\mathbf{r}')\, G(\mathbf{r}, \mathbf{r}') = -1. \tag{3}$$

We should note that the $E_{\rm XC}[n]$ functional given by equation (1) is formally exact and the approximation (2) for the ipcf does not imply any restriction for the types of system we can

study with this approach. So, the formalism can be used to describe a general realistic system, although we will only study jellium surfaces. It has been shown that the scaling hypothesis (2) is actually a good approximation for bulk systems [39]. Moreover, the WDA fulfils some exact features beyond the scope of the LDA and GGA. First, the WDA XC potential has the correct $-1/r$ asymptotic behaviour for finite systems [13]. Second, the WDA is designed to capture effects due to the inhomogeneity of the electron densities [40–42], where the LDA/GGA is not well defined. Finally, although they do not cancel exactly, the self-interaction errors are much smaller than in the case of LDA/GGA. This explains why the WDA offers a superior performance when studying, for instance, transition-metal and rare-earth materials [43–45].

Unfortunately, since the ipcf for an homogeneous electron gas has spherical symmetry, the WDA ipcf $G^{\mathrm{WDA}}(\mathbf{r}, \mathbf{r}')$ is also spherically symmetric. This is not a serious drawback when considering bulk materials and finite systems (atoms, molecules, clusters). However, it has important consequences in semi-infinite systems like surfaces and slabs. In fact, for a metal surface the ipcf centred deep inside the vacuum shows a large deformation [46] that cannot be described by the WDA. As a result, the corresponding WDA XC potential behaves as $-1/2(z - z_0)$ [35].

This limitation can be circumvented by a suitable modification of the WDA (mWDA) [15, 16] which provides a more realistic description of the ipcf for semi-infinite electron systems. In the mWDA, $G(\mathbf{r}, \mathbf{r}')$ is approximated by the expression

$$G(\mathbf{r}, \mathbf{r}') \simeq G_{\mathrm{hom}}(\tilde{n}(\mathbf{r}), |\mathcal{H}(\mathbf{r})\,(\mathbf{r}' - \mathbf{r})|), \tag{4}$$

where now $\mathcal{H}(\mathbf{r})$ is a deformation matrix and $\tilde{n}(\mathbf{r})$ is the weighted density. For bulk and finite systems, $\mathcal{H}(\mathbf{r})$ is set to unity, hence recovering the original WDA. However, for semi-infinite and slab geometries, the deformation matrix is given by

$$\mathcal{H}(\mathbf{r}) = \begin{pmatrix} h^{-1/2}(\mathbf{r}) & 0 & 0 \\ 0 & h^{-1/2}(\mathbf{r}) & 0 \\ 0 & 0 & h(\mathbf{r}) \end{pmatrix} \tag{5}$$

(we always consider that z is the coordinate perpendicular to the surface or the slab). Therefore, for each point $\mathbf{r}$ we need to evaluate $\tilde{n}(\mathbf{r})$ and the deformation function $h(\mathbf{r})$. This can be done by imposing the sum rule (3) and the approximate ansatz for the shape of the ipcf at a metal–vacuum interface,

$$\int \mathrm{d}\mathbf{r}' \, \frac{(z' - z)^2}{|\mathbf{r}' - \mathbf{r}|^2} \, n(\mathbf{r}') \, G(\mathbf{r}, \mathbf{r}') = -\frac{1}{3}. \tag{6}$$

Note that both $\tilde{n}(\mathbf{r})$ and $h(\mathbf{r})$ are auxiliary quantities that need to be calculated for each point in real space in each iteration of the self-consistent calculation. The corresponding XC potential $v_{\mathrm{XC}}(\mathbf{r})$ is then expressed by the analytical functional differentiation of (1). By construction, the mWDA XC potential recovers the right asymptotic behaviour $-1/4(z - z_0)$ at a metal surface [15]. Moreover, for a simple jellium metal surface, the translational invariance along the xy plane allows a great simplification of all the above expressions [16] and a fully self-consistent mWDA-KS calculation is only slightly more expensive than using the standard WDA. For practical purposes, in the evaluation of $G_{\mathrm{hom}}(n, |\mathbf{r} - \mathbf{r}'|)$ we use the parameterization proposed in [12] that ensures the required numerical stability for the evaluation of $v_{\mathrm{XC}}(\mathbf{r})$ deep inside the vacuum. This quite simple parameterization fits very well other more sophisticated forms [47, 48] in the range of metallic densities. The XC energies of the homogeneous electron gas, when required, are calculated using the parameterization by Perdew and Wang [49].

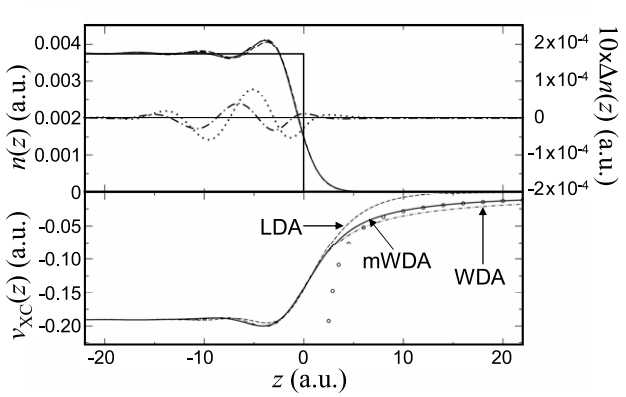

Figure 1. Upper panel: self-consistent Kohn–Sham densities for a jellium surface ($r_s = 4$) using the mWDA (——), the WDA (— · —), and the LDA (- - - -) functionals. The additional dotted and dash–dotted lines show the difference $10 \times [n(z)^{\mathrm{mWDA}} - n(z)^{\mathrm{LDA}}]$ and $10 \times [n(z)^{\mathrm{mWDA}} - n(z)^{\mathrm{WDA}}]$, respectively. Lower panel: the three corresponding v_{XC} potentials for the same jellium system. The open circles represent the asymptotic image-like behaviour $-1/4(z - z_0)$ with $z_0 = 1.2$.

3. Surface ground-state properties

To mimic a metal–vacuum interface, we have considered finite jellium slabs with thickness L ranging from $8r_s$ to $16r_s$. Although $L = 8r_s$ is enough to describe qualitatively the surface properties, specific numerical values depend very sensitively on L due to the filling of new sub-bands that appear when increasing L. Therefore, *pure* surface properties that actually correspond to a semi-infinite system have to be obtained by careful numerical extrapolation procedures [50, 51] of the data corresponding to finite slab geometries.

As a first illustration, in the upper panel of figure 1 we compare the electron density profiles obtained after self-consistent KS calculations using the LDA, the WDA, and the mWDA for an $r_s = 4$ metal surface. We may see that there are only marginal differences between the WDA and the mWDA densities, hence ensuring that the modification of the shape of the ipcf given by the mWDA is only important far outside the bulk. Therefore, the small differences with respect to the LDA density (that mainly appear at the first Friedel peak with slight depressions in the remaining Friedel oscillations) can be solely attributed to changes in the XC potential in the interface that were already described by the standard non-local WDA. This can be observed in the lower panel of figure 1, where we plot the corresponding self-consistent XC potentials. As expected, the only noticeable discrepancy between the WDA and the mWDA potentials is the different asymptotic behaviours: $-1/2z + \mathrm{o}(z^2)$ for the WDA and $-1/4z + \mathrm{o}(z^2)$ (the correct one) for the mWDA.

A simple way to quantify the differences between several self-consistent densities is the evaluation of the work function (defined as the difference between the vacuum and the Fermi energy levels). The work function has an XC contribution (which is a bulk property and does not depend on the functional model since the LDA, WDA, and mWDA are exact in the homogeneous limit) plus an electrostatic one determined by the electron density profile [25]. As a consequence (see table 1), the WDA and mWDA work functions are practically the same, whereas the almost negligible deviation (less than 0.1 eV) with respect to the LDA values are just the consequence of the small differences between the self-consistent densities described above.

Table 1. Work functions Φ (in eV) for simple metal surfaces. The work function is rather insensitive to the functional model and there are not any relevant discrepancies between the non-local WDA and mWDA results.

r_s	2	3	4	5	6
mWDA	3.87	3.41	2.95	2.57	2.27
WDA	3.90	3.42	2.95	2.57	2.27
LDA	3.79	3.36	2.90	2.53	2.24

Table 2. The surface energy and its contributions (in erg cm^{-2}) calculated on different self-consistent Kohn–Sham density profiles. σ_{tot} is the total surface energy, σ_S and σ_{el} are the kinetic and electrostatic contributions, respectively. The XC contributions, σ_{XC}, are evaluated with different functional approximations (LDA, WDA, and mWDA), and the corresponding self-consistent values are highlighted. σ_{EXX} is the exchange contribution to the surface energy calculated from the exact expression in terms of Kohn–Sham orbitals. Finally, the last column (σ_{XC}^{ACFDT}) is the sum of σ_{EXX} and the ACFDT correlation contribution reported in [51] (both evaluated using LDA wavefunctions as an input).

r_s	σ_{tot}	σ_S	σ_{el}	σ_{XC}^{LDA}	σ_{XC}^{WDA}	σ_{XC}^{mWDA}	σ_{EXX}	σ_{XC}^{ACFDT}
Self-consistent LDA density								
2	−869	−5496	1275	**3355**	3315	3337	2624	3422
3	222	−704	163	**764**	763	770	526	788
4	162	−140	41.4	**262**	264	267	157	273
5	97	−30.4	16.7	**111**	114	116	57.0	116
Self-consistent WDA density								
2	−913	−5490	1269	3342	**3312**	3334	2627	
3	220	−705	166	761	**760**	767	525	
4	164	−142	44.7	260	**262**	265	155	
5	99	−31.9	19.5	109	**112**	114	55.1	
Self-consistent mWDA density								
2	−891	−5494	1273	3358	3312	**3333**	2633	
3	227	−708	168	766	761	**768**	528	
4	167	−143	45.1	263	263	**266**	158	
5	101	−33.1	19.6	112	113	**115**	57.4	

Once we have evaluated the self-consistent density profiles it is possible to calculate the surface energy σ_{tot} and its corresponding contributions: kinetic (σ_S), electrostatic (σ_{el}), and exchange–correlation (σ_{XC}). Since the mWDA can be regarded as the most accurate functional method to evaluate the XC potential (and, consequently, the electron density) at a metal surface, we can estimate the errors appearing in σ_S and σ_{el} due to simpler approximations like the LDA. As we can see in table 2, there are some differences if we consider σ_S and σ_{el} separately. However, they tend to cancel each other, resulting in a marginal difference (of the order of 1 erg cm^{-2}) in the total surface energies.

Actually, the discrepancies between the total LDA, WDA, and mWDA surface energies (also shown in table 2) are mainly due to the different nature of the approximations to the XC energy which, on the other hand, is also quite stable under changes in the self-consistent density profiles. The WDA lowers the LDA results for σ_{XC} with the exception of the low-density limit (higher r_s). The mWDA trend is the opposite since, except for $r_s = 2$, the mWDA gives greater XC contributions than the LDA. Nevertheless, the discrepancies among the different results are not dramatic, thus confirming the fact that jellium surface energies

are very robust quantities regardless of the functional approximation used [52]. Then, this fair agreement between the self-consistent mWDA and LDA energies can be seen as a further confirmation of the reliability of density functional methods when evaluating surface energies. In fact, it is now believed [53–55] that existing diffusion quantum Monte Carlo results for the surface energy [46] are contaminated by some convergence problems. Thus, the most reliable XC contributions to the jellium surface energies have been obtained so far using techniques based on time-dependent DFT [50, 51, 53]. As it is explained in detail in these references, the exchange contribution is calculated using the exact expression in terms of the occupied KS orbitals (which we will label as σ_{EXX}), whereas the correlation part is obtained through the adiabatic-connection fluctuation–dissipation theorem (ACFDT) [56]. The total XC contribution to the surface energy so obtained, $\sigma_{\mathrm{XC}}^{\mathrm{ACFDT}}$, is greater than the LDA and mWDA ones, but the deviations are always less than 5% (a rather small amount considering that the surface energy is actually a binding energy).

However, since accurate diffusion quantum Monte Carlo results are still lacking, the ACFDT prescription does not provide the definitive answer to the long-standing surface energy puzzle. The two main drawbacks of this method are the absence of self-consistency (the KS orbitals used are generally the LDA ones) and the description of the so-called XC kernel at an approximate level (see the general reviews [7] and [8] for a deeper discussion about the latter). Certainly, the calculations presented in this article cannot give any clue regarding the quality of the XC kernel, but can be useful to quantify the errors due to the use of LDA orbitals when calculating $\sigma_{\mathrm{XC}}^{\mathrm{ACFDT}}$. In this respect, the values of σ_{EXX} are marginally affected if we use mWDA-KS orbitals instead of LDA ones (see table 2). Prospective calculations (the ACFDT is much more expensive to implement than the mWDA) indicate that this is also the case for the ACFDT correlation contribution. Considering the above discussion about the stability of the kinetic and electrostatic contributions, we can conclude that the errors related to the use of LDA orbitals in prescriptions based on time-dependent DFT to evaluate surface energies are not important at all. However, we must point out that this does not mean that LDA orbitals were appropriate if we intend to evaluate excited-state properties. The ACFDT energies are integrated quantities, but specific spectral properties are affected by the properties of isolated KS eigenvalues and eigenenergies which, as commented in the introduction, depend on the quality of the XC potential. The discussion of the properties of such an XC potential will be the topic of the next section.

4. XC potential and image-like behaviour

The term image potential designates the asymptotic form of the potential that an electron feels when it is placed in front of a metallic surface. This name is taken from the classical analogy of a test charge interacting with its image charge inside the metal. One can obtain this same asymptotic behaviour when considering the quantum case, as Bardeen showed in 1940 [57]. The validity of this asymptotic form for the XC potential was demonstrated by Almbladh and von Barth [23] and Sham [24] but, despite this analogy, one should not forget that a fictitious KS electron is not the same as an interacting test charge placed outside a metal surface. The rigorous study of the interaction between an electron placed outside a surface with the bulk electrons requires the use of many-body theory, in which the additional electron has to be considered as a quasiparticle excitation [31, 58, 59]. Deisz and collaborators [58] have shown that for a jellium surface the local, real and static XC potential $v_{\mathrm{XC}}(z)$ is a good approximation to the real part of the non-local, complex and dynamic self-energy that a quasielectron feels outside the surface. Thus, an approximate $v_{\mathrm{XC}}(z)$ exhibiting the right asymptotic behaviour can be used to obtain a first approximation to the wavefunction and energy of this quasiparticle.

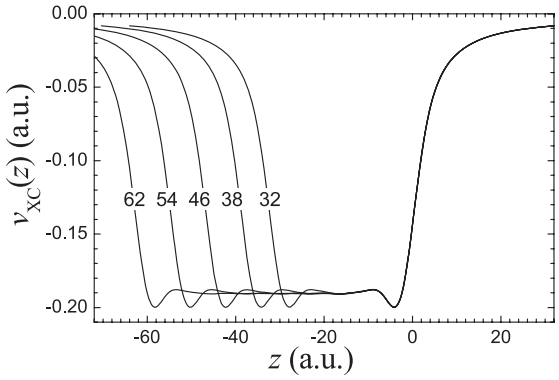

Figure 2. XC potentials, $v_{XC}(z)$, for jellium slabs ($r_s = 4$) with different slab thickness (shown in the figure in au). In all cases the right jellium edge is located at $z = 0$. Note that, at a first glance, the XC potential outside the surface does not depend on the slab thickness.

On the other hand, a proper $v_{XC}(z)$ should be used when evaluating the properties of neutral excitations like surface plasmons. However, since these collective excitations are confined in the metal/vacuum interface, it is likely that the image-like behaviour will have a minor role when determining surface plasmon properties [60].

The image-like behaviour of the XC potential

$$v_{XC}(z) = -\frac{1}{4(z - z_0)} + \frac{c}{z^3} + \cdots, \tag{7}$$

is due to long-range Coulomb correlations that, of course, are not described by the LDA and extensions thereof. These approximations incorrectly transmit into v_{XC} the exponential shape of the density outside a metal surface. As commented, the non-local weighted density approximation WDA is able to provide a behaviour proportional to z^{-1} but with a wrong factor, and the mWDA is the only explicit functional approximation that shows the right asymptotic behaviour (7). These features have been already illustrated in figure 1, but now we wish to present a deeper study focused on the effective image plane position z_0, which is obtained by fitting the mWDA potential deep inside the vacuum by the expression (7).

First of all, for each r_s we need to determine the dependence of z_0 versus the thickness L of the jellium slab used to mimic an actual jellium/vacuum interface. As we may see in figure 2, the asymptotic behaviour of v_{XC} seems to be completely independent of the slab thickness. However, z_0 is a very delicate quantity, as reflected by the fact that changes of five units in the fourth significant digit in v_{XC} leads to one unit changes in the second significant digit of z_0. This implies that we have to face not only the unavoidable numerical uncertainties in the fitting procedure, but also the oscillatory behaviour exhibited by z_0 when increasing the slab widths (see figure 3). The amplitudes of such oscillations seem to be rather independent of the jellium mean density except for $r_s = 2$, where the fitting procedure is not fully stable. In fact, those amplitudes are of the same order of magnitude as the fitting uncertainties. As a result we can obtain (with the exception mentioned for $r_s = 2$) the final value of z_0 with a reasonable relative error, as presented in table 3.

It is interesting to compare z_0 with its semiclassical counterpart, z_0^c, defined as the centroid of the induced charge at the metal surface due to the quantum response to the presence of a classical test charge located deep inside the vacuum. This test charge generates an electric field that is practically uniform at the surface, thus the evaluation of z_0^c can be done preserving the translational symmetry of the problem [60–62]. In figure 3 we compare z_0 and z_0^c for

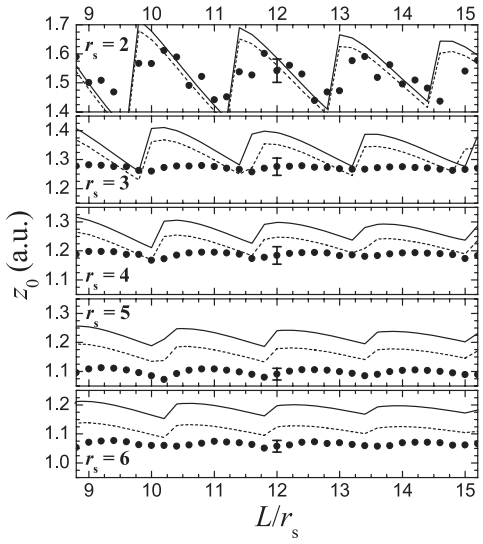

Figure 3. The image-plane position z_0 (full circles), found from the mWDA $v_{XC}(z)$ asymptotic behaviour, is compared with the centroid z_0^c of the density induced by an external test-charge for different slab thicknesses (L) and bulk densities. z_0^c is obtained using the mWDA (——) and the LDA (– – –). Note that, regardless of the specific geometry, z_0 is always less than z_0^c. Typical error bars related to the fitting procedure required to obtain z_0 are also included.

Table 3. The extrapolated values of the mWDA image-plane position z_0 compared with the semiclassical counterpart z_0^c obtained with the mWDA and LDA. We also include the image-plane position from a LDA-based semi-empirical matching procedure [33] reported in [36]. The marginal discrepancies between our LDA values and those reported previously [61, 62] are solely due to the use of different parameterizations of the homogeneous electron gas XC energy.

r_s	z_0 (fit from v_{XC}^{mWDA})	z_0^c (mWDA)	z_0^c (LDA)	Matching
2	1.53 ± 0.06	1.56 ± 0.02	1.54 ± 0.02	1.56
3	1.28 ± 0.04	1.35 ± 0.02	1.31 ± 0.02	1.37
4	1.17 ± 0.04	1.25 ± 0.02	1.22 ± 0.02	1.28
5	1.10 ± 0.03	1.21 ± 0.02	1.17 ± 0.02	1.23
6	1.07 ± 0.03	1.19 ± 0.02	1.13 ± 0.02	1.19

different r_s and slab thicknesses L, z_0^c being obtained using the LDA and the mWDA. As we may see, the mWDA non-local treatment of XC effects increases the value of z_0^c with respect to the LDA, a trend that is also exhibited by the standard WDA [37]. However, this mWDA z_0^c is clearly greater than z_0. In other words: under the mWDA, the centroid of the induced density by an external classical test-charge z_0^c is greater than the position of the image-plane z_0 given by the asymptotic behaviour of the XC potential. Moreover, the difference between both quantities increases as the bulk mean density decreases. The final extrapolated values are presented in table 3. For completeness, we also include the image-plane position obtained by Kiejna [36] using a semi-empirical recipe proposed by Serena and collaborators [33]. Under this scheme, the correct image-like limit of the XC potential is extrapolated from the LDA one at the metal/vacuum interface through a self-consistent matching procedure. Note that this prescription gives quite similar results as the mWDA centroid z_0^c and, therefore, they are greater than the mWDA image-plane position z_0.

These quantitative differences between z_0 and z_0^c have been already shown [59, 63–65] by obtaining the asymptotic behaviour of $v_{XC}(z)$ using many-body perturbation theory. This procedure (see the review [31] for further details) allows a reliable description of the subtle correlation effects that appear in a surface system. However, a complete comparison between the mWDA and the many-body results is not possible since both approaches behave differently in the bulk limit, where the mWDA is exact by construction. It is very likely that the actual value of z_0 will lie between the mWDA values and the many-body ones reported in [59, 63, 64], but this is still an open issue. Nevertheless, bearing in mind that the mWDA is based on a modelization that depends explicitly on the density, its capability to describe at least qualitatively the different nature of z_0 and z_0^c is a success of this functional approximation.

5. Conclusions

In this paper we have implemented, for the first time, a DFT calculation of the ground-state properties of a metal surface using a non-local approximation (mWDA) to the XC energy functional whose functional derivative is exact in the bulk limit and, at the same time, exhibits the proper image-like asymptotic behaviour outside the surface. As expected, the self-consistent density so obtained is very similar to the one obtained using the local density approximation. As a by-product, we have assessed the quality of the LDA approximation as a starting point of sophisticated calculations of the surface energy, confirming its reliability.

The image-plane position z_0 and the centroid of the induced density by an external test-charge z_0^c given by the mWDA show the same trends as the ones obtained using the much more involved many-body perturbation theory. Although we believe that the mWDA still overestimates the actual value of z_0, further many-body studies are required to confirm this point since the actual behaviour of the XC potential is still under debate [66]. Nevertheless, the calculations presented in this paper show that the mWDA self-consistent functional approximation is an optimal starting point for the evaluation of excited-state properties either using many-body perturbation theory or time-dependent density functional theory.

Acknowledgments

The authors were partially supported by the Spanish Ministry of Education and Science through the project FIS2004-05035-C03, the Ramón y Cajal Program (PGG) and an FPU predoctoral grant (JJ). We benefited from discussions with Professor P Tarazona, Professor J F Dobson, Professor R W Godby, and Dr Julio Fernández-Sánchez.

References

[1] Kohn W and Sham L 1965 *Phys. Rev.* **140** A1133
[2] Hohenberg P and Kohn W 1964 *Phys. Rev.* **136** B864
[3] Jones R O and Gunnarsson O 1989 *Rev. Mod. Phys.* **61** 689
[4] Fiolhais C, Nogueira F and Marques M (ed) 2003 *A Primer in Density Functional Theory* (Berlin: Springer)
[5] Perdew J P, Burke K and Ernzerhof M 1996 *Phys. Rev. Lett.* **77** 3865
[6] Perdew J P and Kurth S 1998 *Density Functionals: Theory and Applications* ed D Joubert (Berlin: Springer)
[7] Onida G, Reining L and Rubio A 2002 *Rev. Mod. Phys.* **74** 601
[8] Marques M *et al* (ed) 2006 *Time-Dependent Density Functional Theory* (Berlin: Springer)
[9] Alonso J A and Girifalco L A 1978 *Phys. Rev.* B **17** 3735
[10] Gunnarsson O, Jonson M and Lundqvist B I 1979 *Phys. Rev.* B **20** 3136
[11] Alvarellos J E, Tarazona P and Chacón E 1986 *Phys. Rev.* B **33** 6579
[12] Chacón E and Tarazona P 1988 *Phys. Rev.* B **37** 4013

[13] Alonso J A and Cordero N A 1996 *Recent Developments and Applications of Modern Density Functional Theory* ed J M Seminario (Amsterdam: Elsevier)
[14] Palummo M, Onida G, Del Sole R, Corradini M and Reining L 1999 *Phys. Rev.* B **60** 11329
[15] García-González P, Alvarellos J E, Chacón E and Tarazona P 2000 *Phys. Rev.* B **62** 16063
[16] García-González P, Alvarellos J E, Chacón E and Tarazona P 2002 *Int. J. Quantum Chem.* **91** 139
[17] Görling A and Levy M 1994 *Phys. Rev.* A **50** 196
[18] Seidl A, Görling A, Vogl P, Majewski J A and Levy M 1996 *Phys. Rev.* B **53** 3764
[19] Perdew J P, Kurth S, Zupan A and Blaha P 1999 *Phys. Rev. Lett.* **82** 2544
[20] Sánchez-Friera P and Godby R W 2000 *Phys. Rev. Lett.* **85** 5611
[21] Tao J, Perdew J P, Staroverov V N and Scuseria G E 2003 *Phys. Rev. Lett.* **91** 146401
[22] Soler J M 2004 *Phys. Rev.* B **69** 195101
[23] Almbladh C-O and von Barth U 1985 *Phys. Rev.* B **31** 3231
[24] Sham L J 1985 *Phys. Rev.* B **32** 3876
[25] Lang N D and Kohn W 1970 *Phys. Rev.* B **1** 4555
[26] Perdew J P, Burke K and Wang Y 1996 *Phys. Rev.* B **54** 16533
[27] Binning G, García N, Rohrer H, Soler J M and Flores F 1984 *Phys. Rev.* B **30** 4816
[28] de Andrés P, Flores F, Echenique P M and Ritchie R 1987 *Europhys. Lett.* **3** 101
[29] Echenique P M and Pendry R 1978 *J. Phys. C: Solid State Phys.* **11** 2065
[30] Echenique P M, Pitarke J M, Chulkov E V and Rubio A 2000 *Chem. Phys.* **251** 1
[31] García-González P and Godby R W 2001 *Comput. Phys. Commun.* **137** 108
[32] Gunnarsson O and Jones R O 1980 *Phys. Scr.* **31** 394
[33] Serena P A, Soler J M and García N 1986 *Phys. Rev.* B **34** 6767
[34] Ossicini S, Bertoni C M and Gies P 1986 *Europhys. Lett.* **1** 661
[35] Chacón E and Tarazona P 1988 *Phys. Rev.* B **37** 4020
[36] Kiejna A 1991 *Phys. Rev.* B **43** 14695
[37] Alvarellos J E and Chacón E 1992 *Surf. Sci.* **269/270** 590
[38] Chulkov E V, Silkin V M and Echenique P M 1997 *Surf. Sci.* **391** L1217
[39] Rushton P P, Tozer D J and Clark S J 2002 *Phys. Rev.* B **65** 235203
[40] García-González P 2000 *Phys. Rev.* B **62** 2321
[41] Rushton P P, Tozer D J and Clark S J 2002 *Phys. Rev.* B **65** 193106
[42] Clark S J and Rushton P P 2004 *J. Phys.: Condens. Matter* **16** 4833
[43] Marzari N and Singh D J 2000 *Phys. Rev.* B **62** 12724
[44] Wu Z, Cohen R E, Singh D J, Gupta R and Gupta M 2004 *Phys. Rev.* B **69** 085104
[45] Wu Z, Cohen R E and Singh D J 2004 *Phys. Rev.* B **70** 104112
[46] Acioli P H and Ceperley D M 1996 *Phys. Rev.* B **54** 17199
[47] Perdew J P and Wang Y 1993 *Phys. Rev.* B **46** 12947
[48] Gori-Giorgi P, Sacchetti F and Bachelet G B 2000 *Phys. Rev.* B **61** 7353
[49] Perdew J P and Wang Y 1992 *Phys. Rev.* B **45** 13244
[50] Pitarke J M and Eguiluz A 2001 *Phys. Rev.* B **63** 45116
[51] Jung J, García-González P, Dobson J F and Godby R W 2004 *Phys. Rev.* B **70** 205107
[52] Yan Z, Perdew J P, Kurth S, Fiolhais C and Almeida L 2000 *Phys. Rev.* B **61** 2595
[53] Pitarke J M and Perdew J P 2003 *Phys. Rev.* B **67** 045101
[54] Pitarke J M 2004 *Phys. Rev.* B **70** 087401
[55] Hine N, Wood B, Foulkes W M C and García-González P 2006 *Phys. Rev.* B at press
[56] Langreth D C and Perdew J P 1977 *Phys. Rev.* B **15** 2884
[57] Bardeen J 1940 *Phys. Rev.* **58** 727
[58] Deisz J J, Eguiluz A G and Hanke W 1993 *Phys. Rev. Lett.* **71** 2793
[59] White I, Godby R W, Rieger M and Needs R 1998 *Phys. Rev. Lett.* **80** 4265
[60] Liebsch A 1997 *Electronic Excitations at Metal Surfaces* (New York: Plenum)
[61] Lang N D and Kohn W 1973 *Phys. Rev.* B **7** 3541
[62] Weber M and Liebsch A 1987 *Phys. Rev.* B **35** 7411
[63] Eguiluz A and Hanke W 1989 *Phys. Rev.* B **39** 10433
[64] Eguiluz A, Heinrichsmeier M, Fleszar A and Hanke W 1992 *Phys. Rev. Lett.* **68** 1359
[65] Heinrichsmeier M, Fleszar A, Hanke W and Eguiluz A 1998 *Phys. Rev.* B **57** 14974
[66] Horowitz C M, Proetto C R and Rigamonti S 2006 *Phys. Rev. Lett.* **97** 026802